

# Multimodal Chemical Analysis of the Brain by High Mass Resolution Mass Spectrometry and Infrared Spectroscopic Imaging

Elizabeth K. Neumann<sup>1,2†</sup>, Troy J. Comi<sup>2,3†</sup>, Nicolas Spegazzini<sup>2,3</sup>, Jennifer W. Mitchell<sup>2,4,5</sup>, Stanislav S. Rubakhin<sup>1,2,5</sup>, Martha U. Gillette<sup>2,3,4,5</sup>, Rohit Bhargava<sup>1,2,3</sup>, Jonathan V. Sweedler<sup>1,2,5\*</sup>

<sup>1</sup>Department of Chemistry, <sup>2</sup>Beckman Institute for Advanced Science and Technology, <sup>3</sup>Department of Bioengineering, <sup>4</sup>Department of Cell and Developmental Biology, <sup>5</sup>Neuroscience Program, University of Illinois at Urbana-Champaign, Urbana, IL.

<sup>†</sup> Authors contributed equally to this work

\* Corresponding author. Email: jsweedle@illinois.edu. Tel: 217-244-7359

## SUPPORTING INFORMATION

### Table of Contents

Figure S1	Pan sharpening of MS ion images by QCL-IR absorbance images, overview of biological replicate 1 .....	S-2
Figure S2	Pan sharpening of MS ion images by QCL-IR absorbance images, dentate gyrus of biological replicate 1 .....	S-2
Figure S3	Pan sharpening of MS ion images by QCL-IR absorbance images, overview of biological replicate 2 .....	S-3
Figure S4	Pan sharpening of MS ion images by QCL-IR absorbance images, dentate gyrus of biological replicate 2 .....	S-3
Figure S5	Pan sharpening of MS ion images by QCL-IR absorbance images, overview of biological replicate 3 .....	S-4
Figure S6	Pan sharpening of MS ion images by QCL-IR absorbance images, dentate gyrus of biological replicate 3 .....	S-4
Figure S7	Overlay of sharpened ion images for biological replicate 2 .....	S-5
Figure S8	Overlay of sharpened ion images for biological replicate 3 .....	S-6
Figure S9	Hyperspectral score images and midlevel data fusion for biological replicate 2 .....	S-7
Figure S10	Hyperspectral score images and midlevel data fusion for biological replicate 3 .....	S-8
Figure S11	<i>k</i> -means clustering for biological replicate 1, <i>k</i> = 11 .....	S-9
Figure S12	Comparison of <i>k</i> -means clustering for biological replicate 1 .....	S-10
Figure S13	Comparison of <i>k</i> -means clustering for biological replicate 2 .....	S-11
Figure S14	Comparison of <i>k</i> -means clustering for biological replicate 3 .....	S-12
Figure S15	Boxplots of potassium and sodium Adducts. ....	S-13

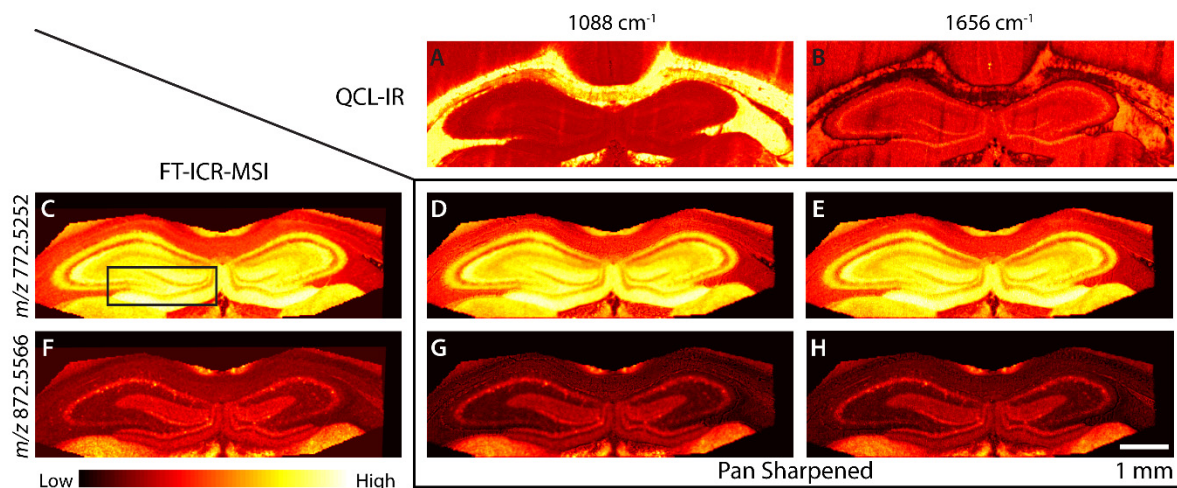


**Figure S1.** Biological replicate 1. Pan sharpening of mass spectrometry (MS) ion images by quantum cascade laser (QCL-IR) absorbance images. (A) QCL-IR image of the hippocampus displaying absorbance at the ester band ( $1088\text{ cm}^{-1}$ ). (B) QCL-IR image of the amide II band ( $1656\text{ cm}^{-1}$ ). (C) Matrix-assisted laser desorption/ionization-Fourier transform ion cyclotron resonance (MALDI-FT-ICR) MS ion image of  $[\text{PC } 40:6 + \text{K}]^+$  ( $m/z\ 772.5252$ ). The boxed region corresponds to the magnified images presented in Figure S2. (D, E) Ion image of  $[\text{PC } 40:6 + \text{K}]^+$  pan sharpened with the (D) ester band or the (E) amide II band. (F) MALDI-FT-ICR MS ion image of  $[\text{PC } 34:0 + \text{K}]^+$  ( $m/z\ 872.5566$ ). (G, H) Ion images of  $[\text{PC } 34:0 + \text{K}]^+$  sharpened with the (G) ester band or the (H) amide II band. MSI was acquired with  $25\text{ }\mu\text{m}$  pixel spacing and QCL-IR was acquired with  $5\text{ }\mu\text{m}$  pixel spacing. Labels A-H have the same definitions in subsequent SI figures 2-6.

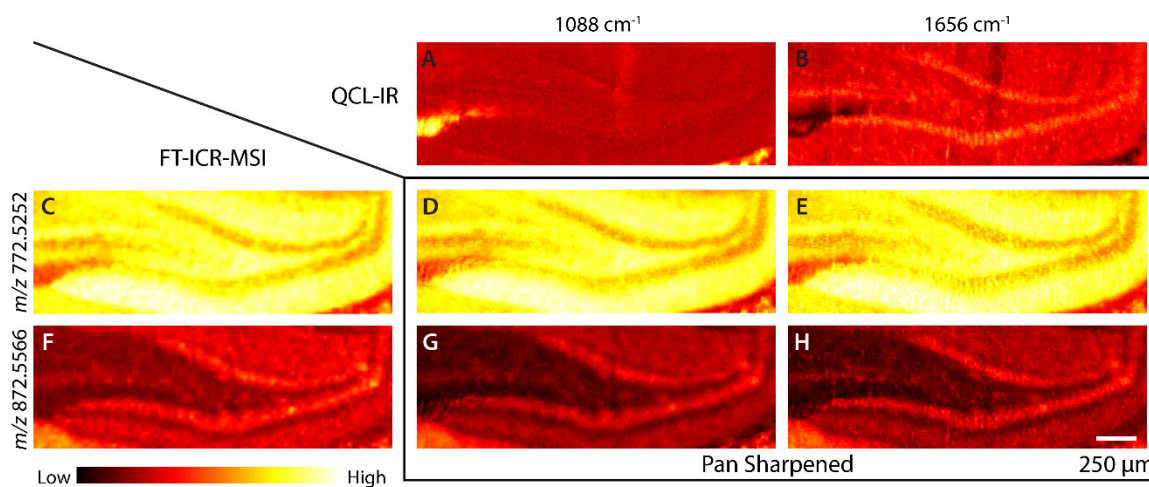


**Figure S2.** Magnified images of Figure S1, focusing on the dentate gyrus (DG).

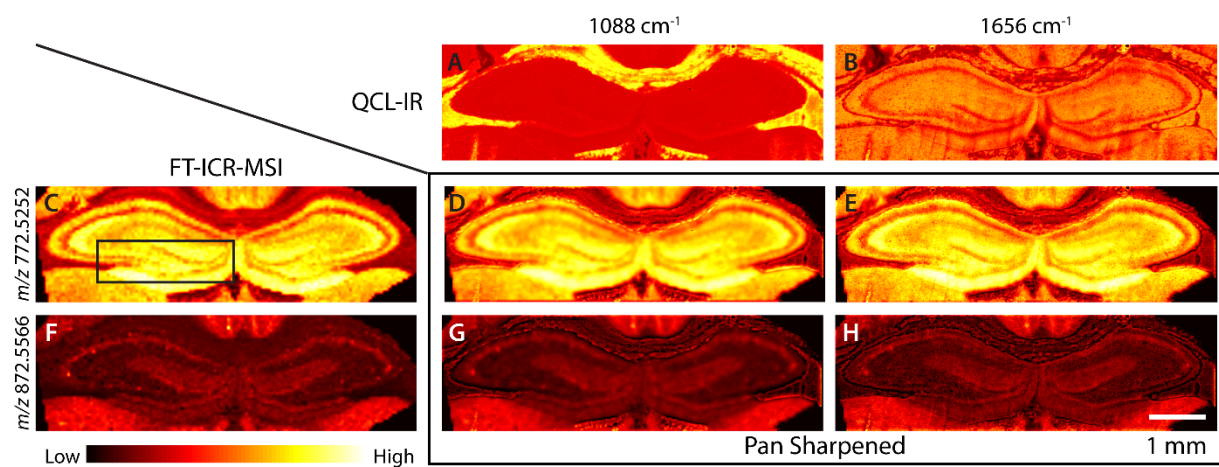


**Figure S3.** Biological replicate 2. In contrast to biological replicate 1, MSI was acquired at 50  $\mu\text{m}$  pixel size. The boxed region in panel C corresponds to the magnified in region in Figure S4.

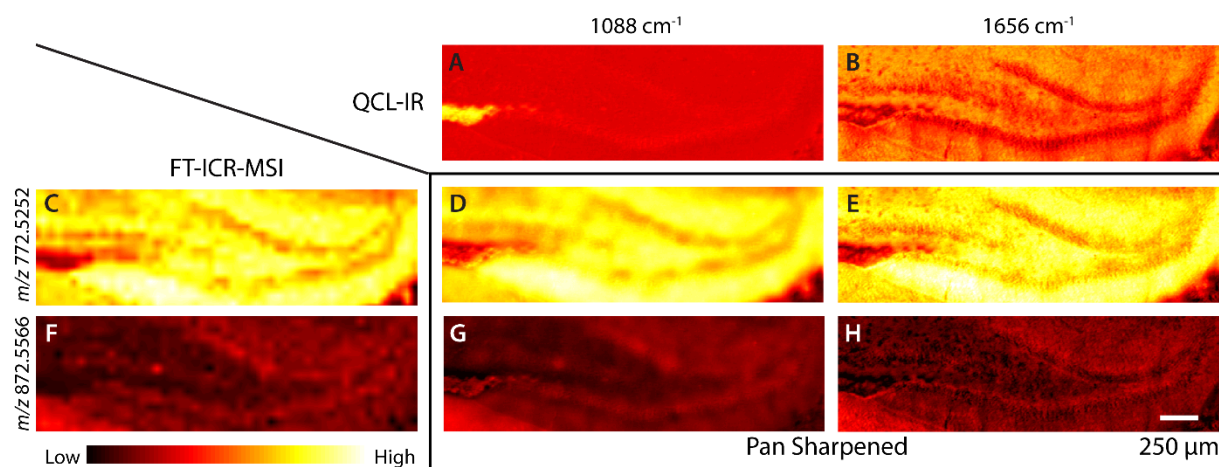


**Figure S4.** Magnified images of Figure S3, focusing on the DG.

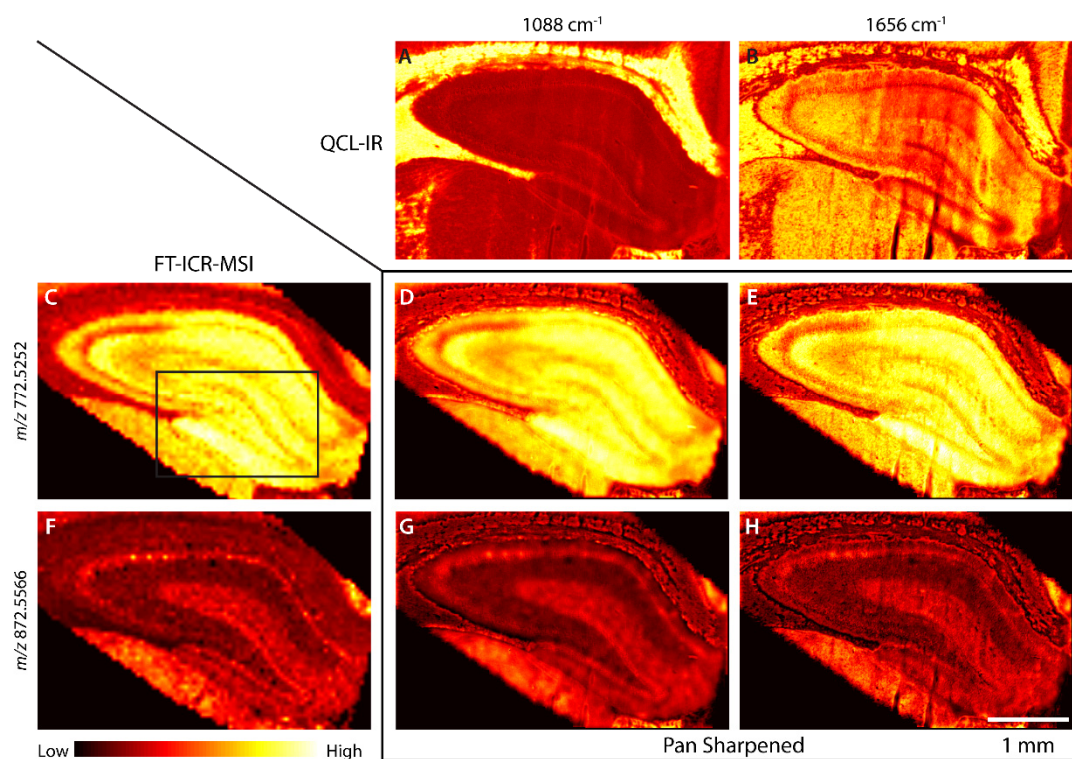


**Figure S5.** Biological replicate 3 with MSI acquired at 50  $\mu\text{m}$  pixel width. Boxed region in Panel C corresponds to the DG region shown in Figure S6.

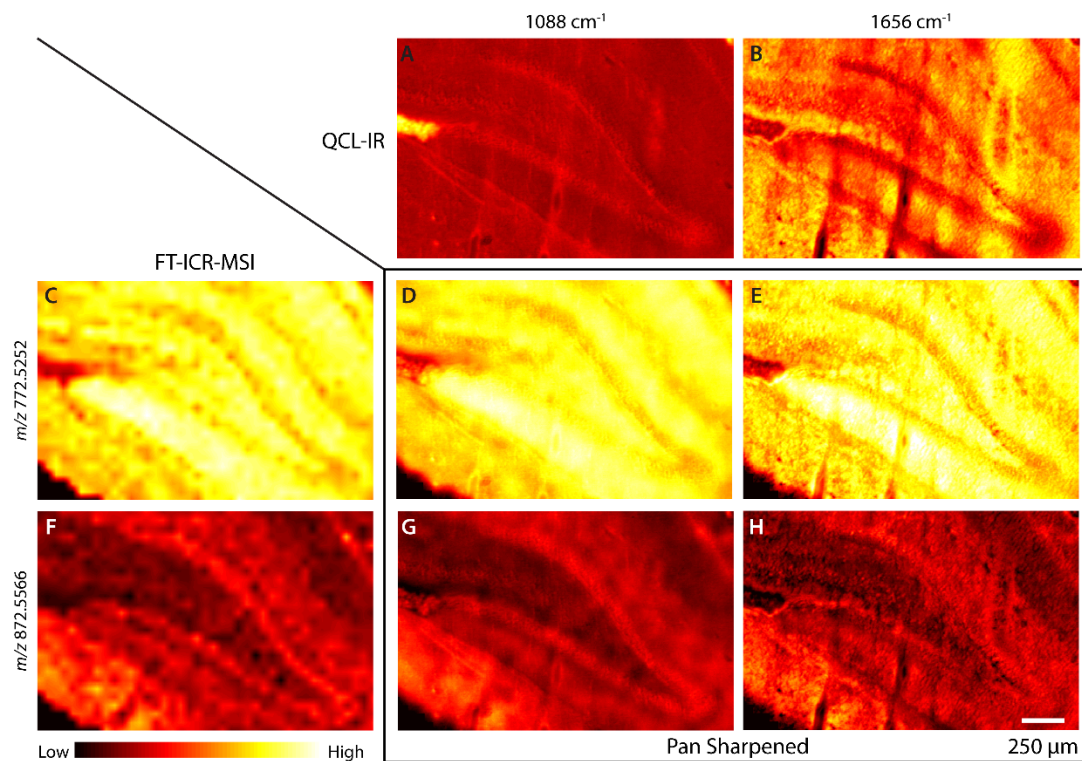


**Figure S6.** Magnified images of Figure S5, focusing on the DG.



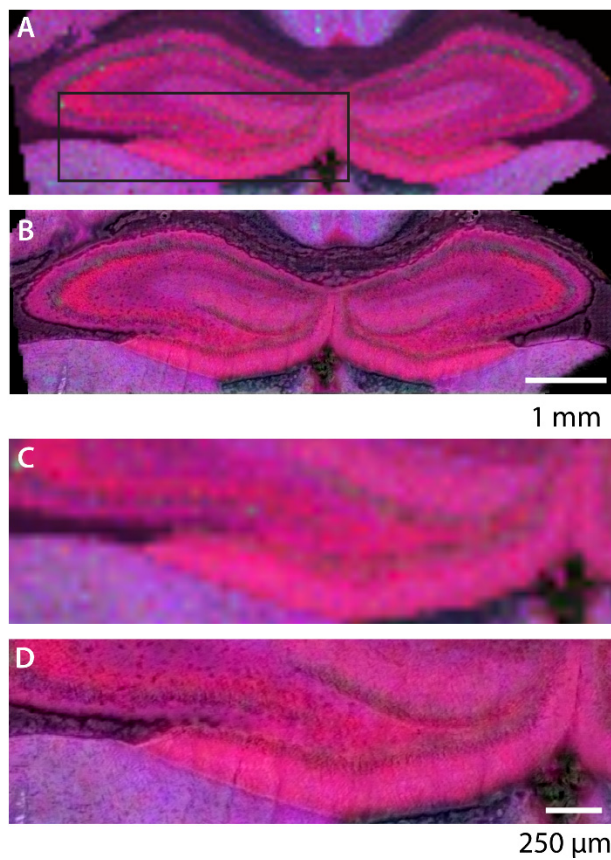


**Figure S7.** Overlay of sharpened ion images for biological replicate 2 of Figure 4. The red, green and blue channels represent the ion intensities of  $[\text{PC } 32:0 + \text{K}]^+$  (772.5253),  $[\text{PC } 40:6 + \text{K}]^+$  (872.5566), and  $[\text{PC } 34:0 + \text{K}]^+$  (800.5567), respectively. (A) Interpolated MS image of the hippocampus taken at 50  $\mu\text{m}$  spatial resolution. The boxed-in region is magnified in panels C and D. (B) MS image sharpened with QCL-IR image acquired at 1656  $\text{cm}^{-1}$ . (C) Interpolated MS image of hippocampal region containing one end of the CA3 region and the DG. (D) Sharpened MS image of the same area shown in C.

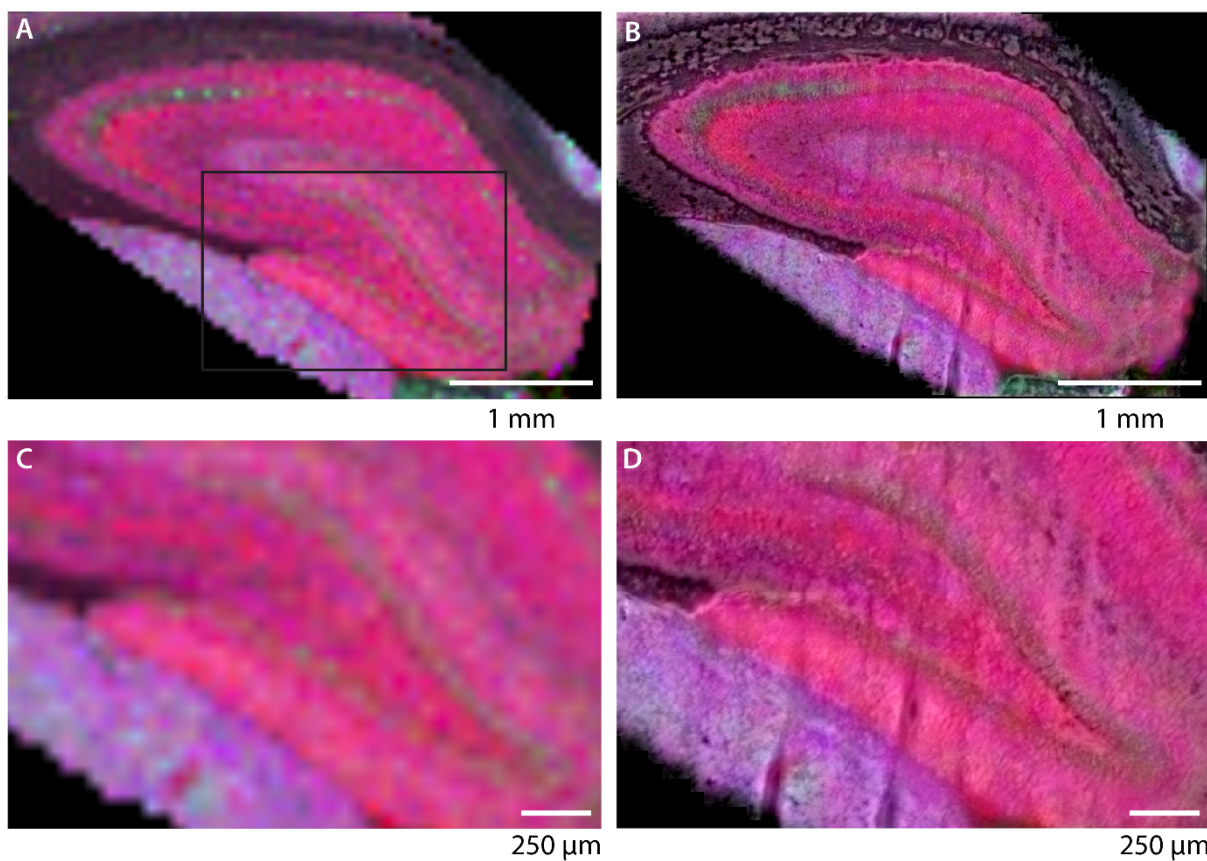


**Figure S8.** Overlay of sharpened ion images for biological replicate 3 of Figure 4. The red, green and blue channels represent the ion intensities of [PC 32:0 + K]<sup>+</sup> (772.5253), [PC 40:6 + K]<sup>+</sup> (872.5566), and [PC 34:0 + K]<sup>+</sup> (800.5567), respectively. (A) Interpolated MS image of the hippocampus taken at 50  $\mu\text{m}$  spatial resolution. The boxed-in region is shown in panels C and D. (B) MS image sharpened with the QCL-IR image acquired at 1656  $\text{cm}^{-1}$ . (C) Interpolated MS image of hippocampal region containing one end of the CA3 region and the DG. (D) Sharpened MS image of the same area shown in C.

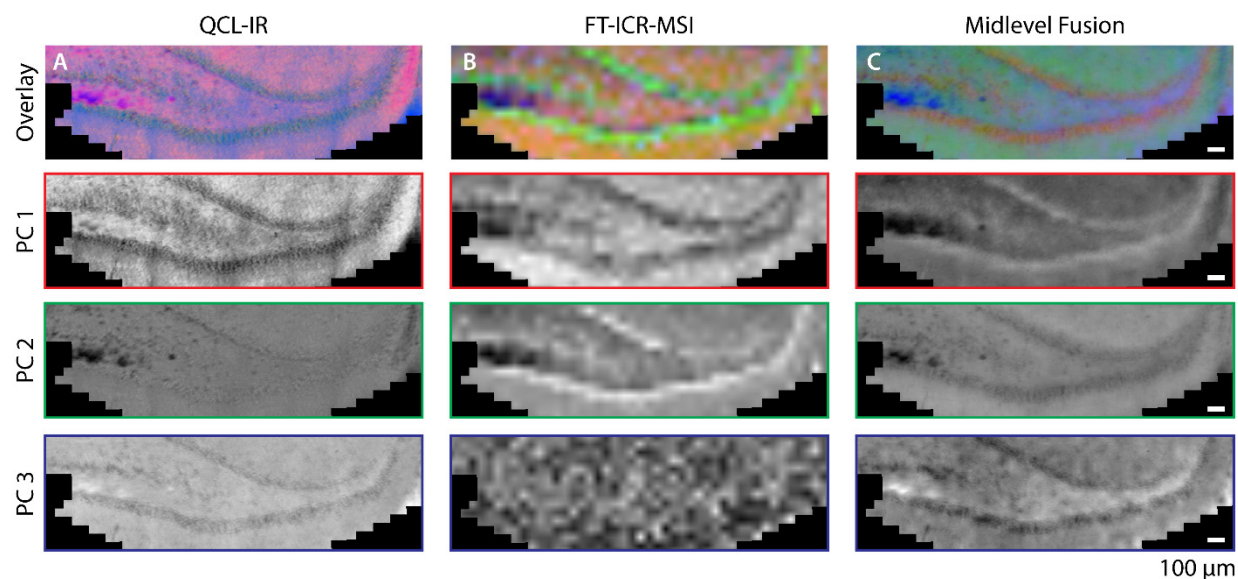


**Figure S9.** Hyperspectral score images of each modality and midlevel data fusion for biological replicate 2. FT-ICR-MSI data were acquired with 50  $\mu\text{m}$  pixel widths. The overlay images (first row) are constructed by mapping principal components 1–3 to red, green and blue, respectively. (A) QCL-IR score image and corresponding single component images. (B) FT-ICR-MSI score image with bilinear interpolation to align with the QCL-IR image area. (C) Midlevel data fusion image of datasets shown in corresponding images in (A) and (B). Hippocampal region, containing one end of the CA3 region and the DG, is depicted.

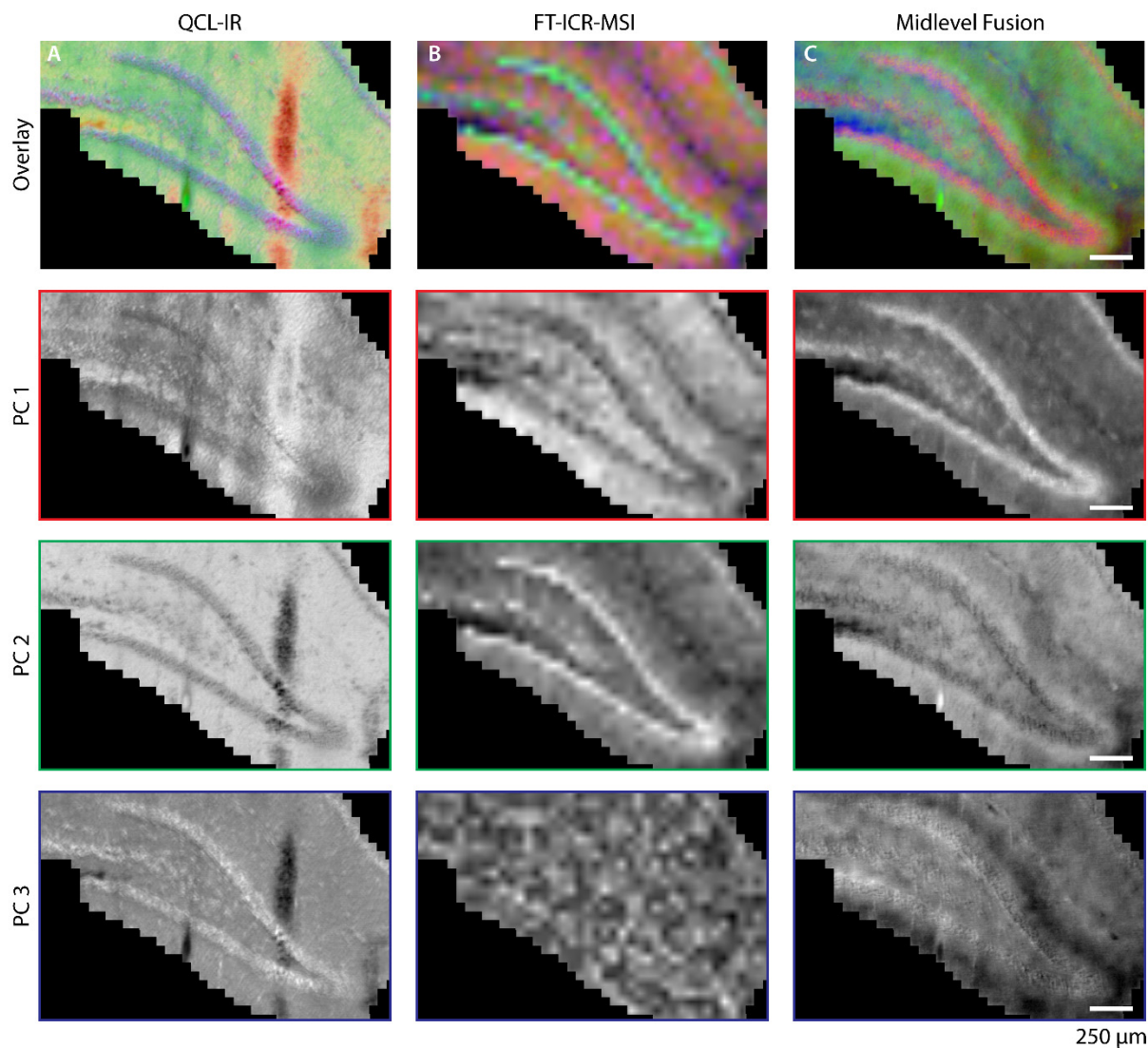


**Figure S10.** Hyperspectral score images of each modality and midlevel data fusion for biological replicate 3. FT-ICR-MSI data were acquired with 50  $\mu\text{m}$  pixel widths. The overlay images (first row) are constructed by mapping principal components 1–3 to red, green and blue respectively. (A) QCL-IR score image and corresponding single component images. (B) FT-ICR-MSI score image with bilinear interpolation to align with QCL-IR image area. (C) Midlevel data fusion image of data sets shown in corresponding images in (A) and (B). Hippocampal region, containing one end of the CA3 region and the DG, is depicted.



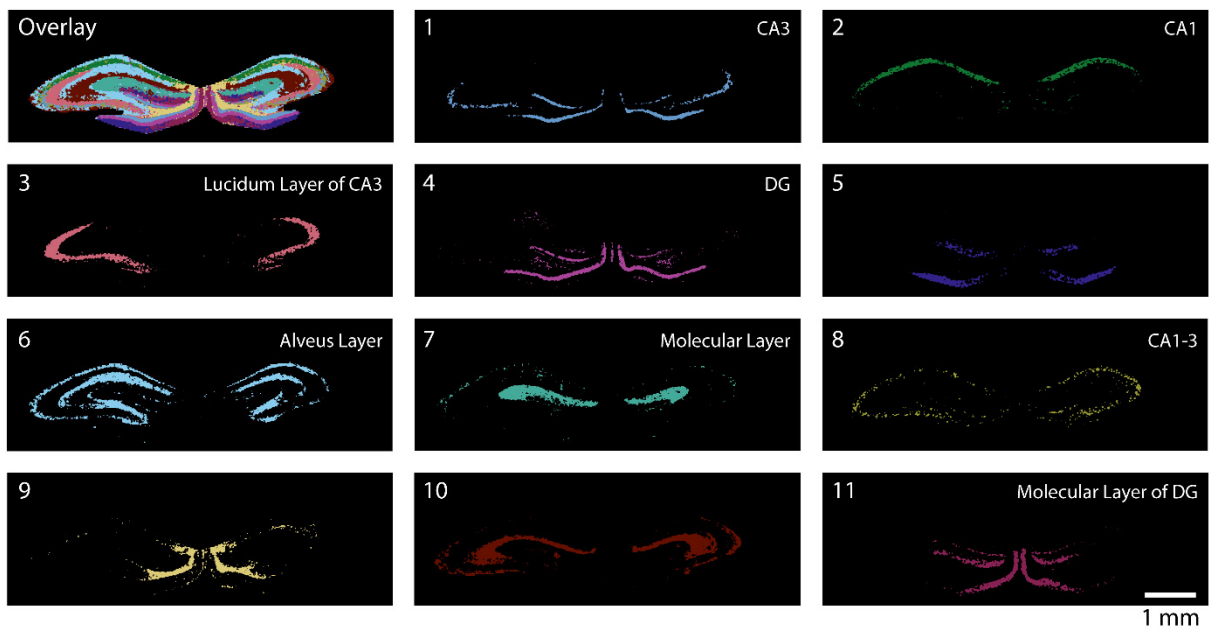


**Figure S11.**  $k$ -means clustering of the midlevel fused datasets of biological replicate 1, with  $k = 11$ . Each pixel in the image is grouped into a defined cluster, signified by a distinct color.  $k = 11$  was found to be the optimum by Davies-Bouldin optimization metric.

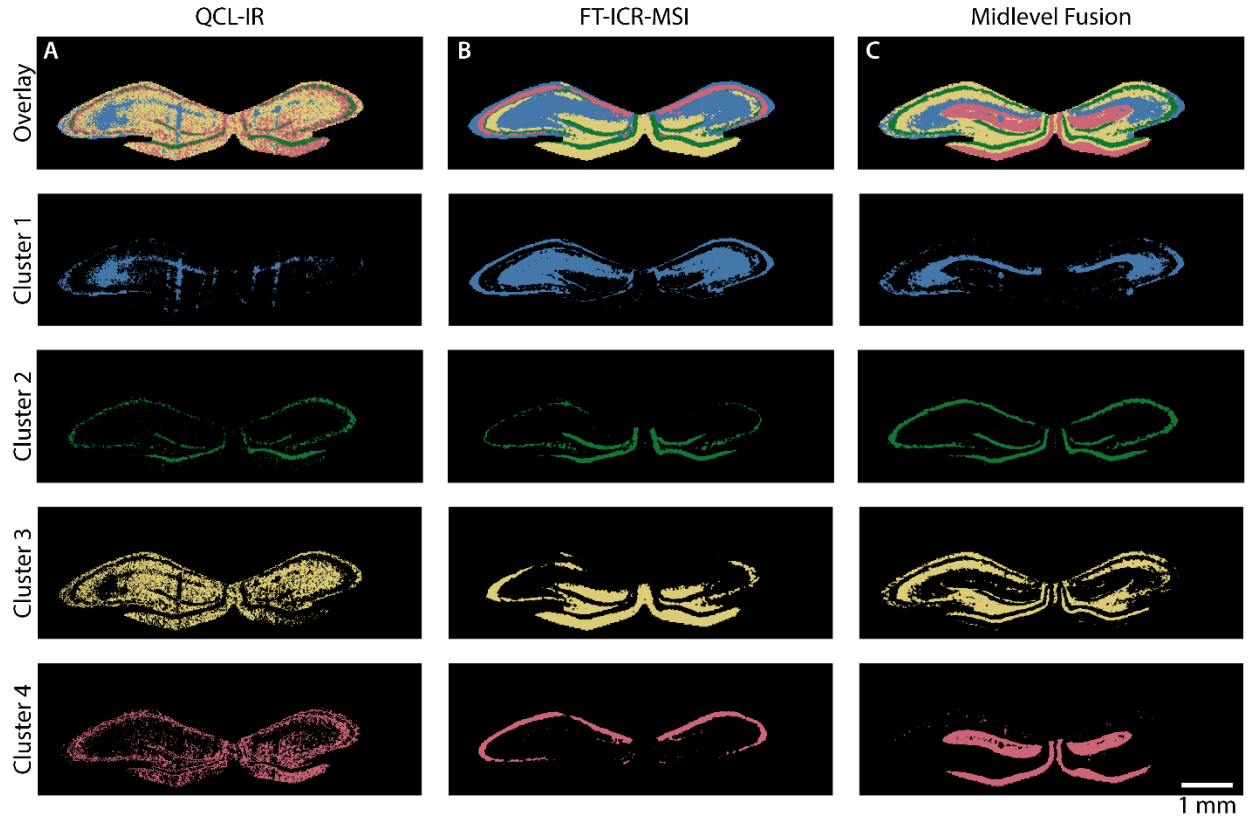


**Figure S12.**  $k$ -means clustering of the (A) QCL-IR, (B) FT-ICR MS, and (C) midlevel fused datasets acquired from biological replicate 1, with  $k = 4$ . Each pixel in the image is grouped into a defined cluster, signified by a distinct color, shown individually in rows 2 through 5. Segments were manually assigned colors to match the highlighted morphology across modalities and biological replicates.

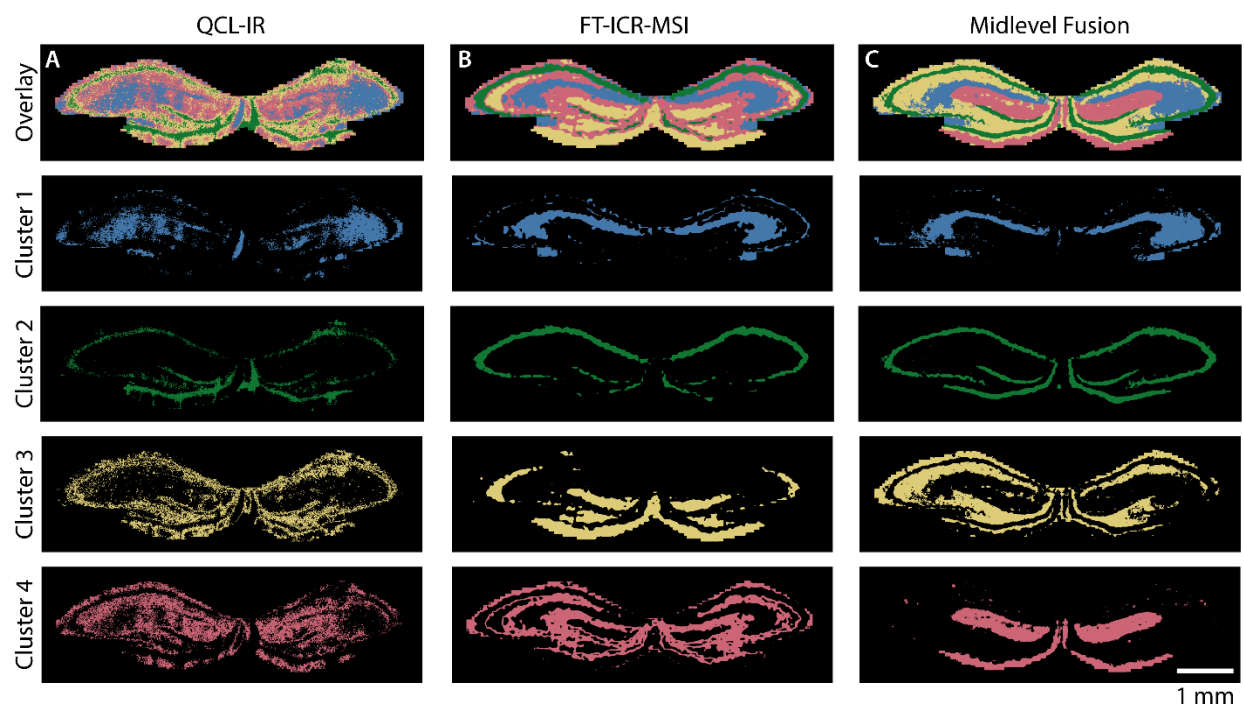


**Figure S13.** *k*-means clustering of the (A) QCL-IR, (B) FT-ICR MS, and (C) midlevel fused datasets of biological replicate 2, with  $k = 4$ . Each pixel in the image is grouped into a separate cluster, signified by a distinct color, shown individually in rows 2 through 5. Segments were manually assigned colors to match the highlighted morphology across modalities and biological replicates.

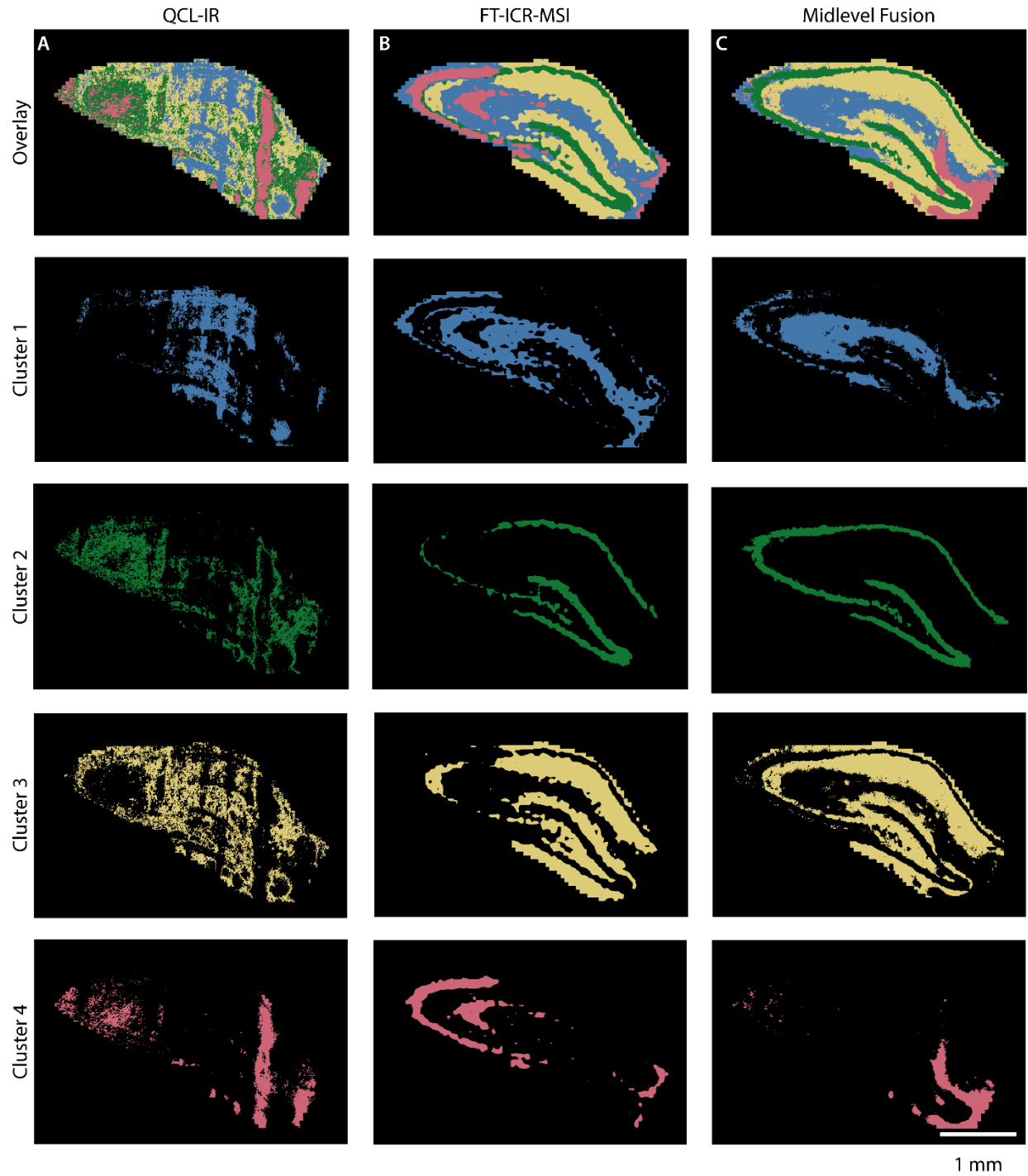


**Figure S14.** *k*-means clustering of the (A) QCL-IR, (B) FT-ICR MS, and (C) midlevel fused datasets of biological replicate 3, with  $k = 4$ . Each pixel in the image is grouped into a separate cluster, signified by a distinct color, shown individually in rows 2 through 5. Segments were manually assigned colors to match the highlighted morphology across modalities and biological replicates. Replicate 3 is a more caudal section of the brain than replicates 1 and 2, as identified by the absence of the granular layer adjacent to the midline (green in segment 2).



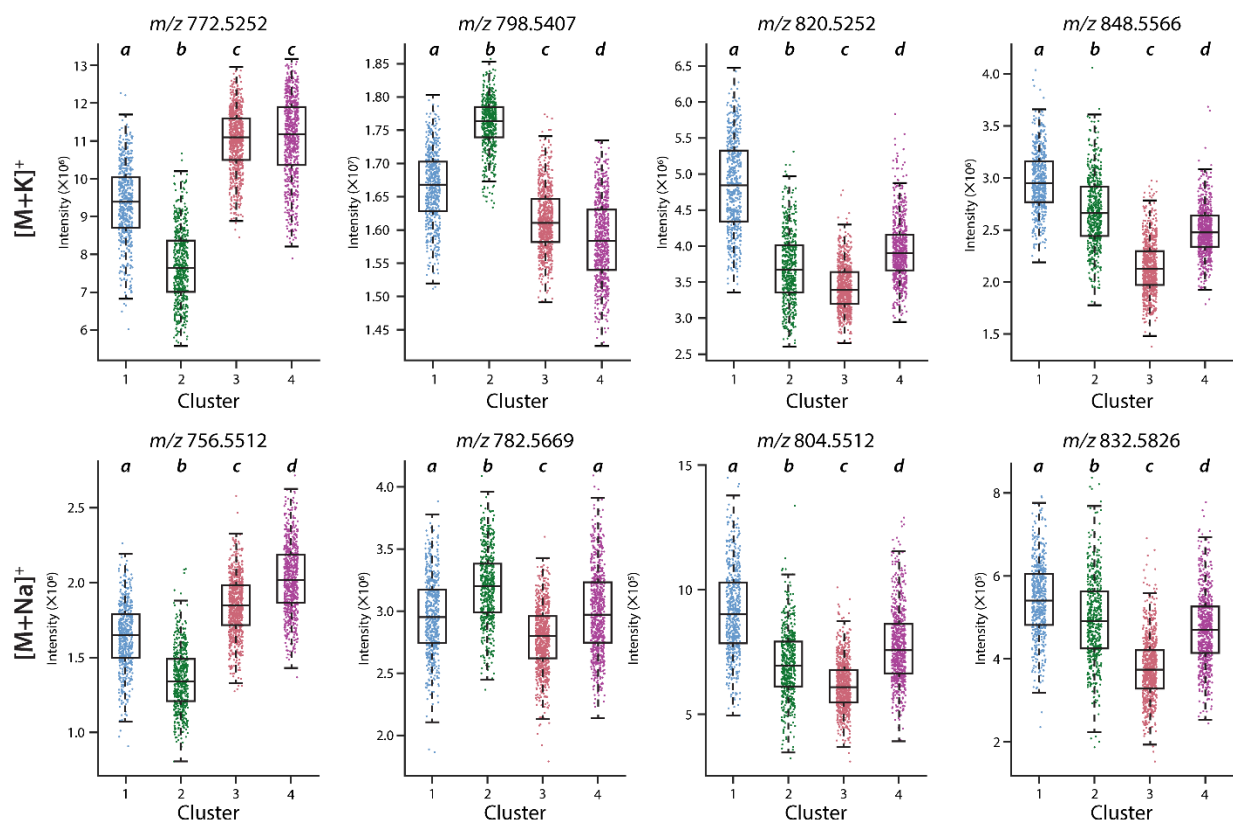


**Figure S15.** Boxplots of potassium and sodium adducts for the ions presented in the main text. The intensity ratios between the salt adducts generally follow the same trend.